ELSEVIER

Journal of Power Sources 111 (2002) 83–89

JOURNAL OF POWER SOURCES

www.elsevier.com/locate/jpowsour

Direct formic acid fuel cells

C. Rice[a], S. Ha[a], R.I. Masel[a,*], P. Waszczuk[b], A. Wieckowski[b], Tom Barnard[b]

[a]*Department of Chemical Engineering, 206 Roger Adams Laboratory, University of Illinois, Box C-3, 600 South Mathews Avenue, Urbana, IL 61801, USA*

[b]*Department of Chemistry, University of Illinois, Urbana, IL 61801, USA*

Received 27 March 2002; accepted 25 April 2002

Abstract

The performance of formic acid fuel oxidation on a solid PEM fuel cell at 60 °C is reported. We find that formic acid is an excellent fuel for a fuel cell. A model cell, using a proprietary anode catalyst produced currents up to 134 mA/cm^2 and power outputs up to 48.8 mW/cm^2. Open circuit potentials (OCPs) are about 0.72 V. The fuel cell runs successfully over formic acid concentrations between 5 and 20 M with little crossover or degradation in performance. The anodic polarization potential of formic acid is approximately 0.1 V lower than that for methanol on a standard Pt/Ru catalyst. These results show that formic acid fuel cells are attractive alternatives for small portable fuel cell applications.

Keywords: Formic acid; Portable power; Micro powergeneration; Polymer electrolyte membrane (PEM) fuel cells

1. Introduction

Polymer electrolyte membrane (PEM) fuel cells are viewed as viable candidates to replace batteries in portable power devices. In this paper, we investigate the use of formic acid as an alternative fuel to methanol in direct fuel cells for portable power applications. The results presented here are the initial findings generated from a newly funded research area for the investigators. Subsequent studies are currently in progress to further explore the direct formic acid fuel cell system. Formic acid is a liquid fuel. It is common to the environment [1,2] and approved for use by the US Food and Drug Administration (FDA) as a food additive [3,4].

Formic acid is a strong electrolyte, hence, is expected to facilitate both electronic and proton transport within the anode compartment of the fuel cell [5]. The theoretical open circuit potential (OCP) or *emf* for a formic acid–oxygen fuel cell, as calculated from the Gibbs free energy, is 1.45 V. The electro-oxidation of formic acid occurs via a dual reaction pathway, reducing the relative percentage of surface poisoning reaction intermediates [6–12]. A reduction in the relative amount of fuel crossover is also expected. A decrease in fuel crossover will (1) improve the overall cell efficiency, and (2) allow the use of high feed concentrations of formic acid, which would in turn facilitate water management [5].

On platinum (Pt), formic acid oxidation occurs via a dual pathway mechanism [6–12]. The most desirable reaction pathway for direct formic acid fuel cells is via the dehydrogenation reaction, which does not form CO as a reaction intermediate. Formic acid oxidation pathway #1 forms CO_2 directly:

$$HCOOH \rightarrow CO_2 + 2H^+ + 2e^- \quad (1)$$

The product CO_2 is formed through step 1, circumventing the adsorbed CO intermediate poisoning step, thereby enhancing the overall turnover rate.

The second reaction pathway via dehydration is somewhat similar to that of methanol oxidation, forming adsorbed carbon monoxide (CO) as a reaction intermediate. Formic acid reaction pathway #2 *dehydration*:

$$HCOOH + Pt^0 \rightarrow Pt{-}CO + H_2O \quad (2)$$

$$Pt^0 + H_2O \rightarrow Pt{-}OH + H^+ + e^- \quad (3)$$

$$Pt{-}CO + Pt{-}OH \rightarrow 2Pt^0 + CO_2 + H^+e^- \quad (4)$$

$$\text{Overall}: \quad HCOOH \Rightarrow CO_2 + 2H^+ + 2e^- \quad (5)$$

In reaction pathway #2, formic acid adsorbs onto the Pt surface forming an intermediate adsorbed CO species (step 2). Adsorbed OH groups (step 3) are required to further oxidize the adsorbed CO intermediate into the gaseous CO_2 end product (step 4). Within the potential range of interest for

* Corresponding author. Tel.: +1-217-333-6841; fax: +1-217-333-5052.
E-mail address: r-masel@uiue.edu (R.I. Masel).

0378-7753/02/$ – see front matter
PII: S0378-7753(02)00271-9

fuel cells, OH groups are not readily adsorbed onto Pt. Therefore, reaction pathway #1 is the desired reaction within the potential range of interest.

For direct formic acid fuel cell, dehydrogenation is the desired reaction pathway, to enhance overall cell efficiency. Anode catalyst selection is pivotal in directing formic acid oxidation to proceed via reaction pathway #1 (reaction 1) [14]. Within the present study a proprietary catalyst was developed and used (UIUC-B). The UIUC-B catalyst selectively enhances the dehydrogenation reaction rate. The catalyst is Pt based, with some other noble metal additives. Further details will be provided in a later paper. In the literature, only one reference was found where formic acid was actually tested in a fuel cell by Savinell and co-workers [13], under different experimental conditions.

The issue of fuel crossover through the membrane, which has plagued direct methanol fuel cells (DMFCs), is not expected to be a limitation for direct formic acid fuel cells, due to its anionic nature (since formic acid partially dissociates to form formate and ions). In a recent paper by White and co-workers, Nafion® has been shown to repel certain molecules based on their ionic charge [15]. The Nafion® polymer consists of a Teflon-like fluorocarbon backbone with side chain fluorocarbon terminating in sulfonic acid ions. Formic acid partially dissociates into formate anions ($HCOO^-$), which are repelled by the sulfonic terminal groups within the Nafion® membrane. Methanol crossover from the anode to the cathode is a significant problem for DMFCs. Hence, a lower methanol feed concentrations is used to limit the amount of crossover. Due to the repulsive characteristics between $HCOO^-$ and the Nafion® membrane, we believe that formic acid crossover through the membrane will be significantly less; thereby permitting the use of significantly higher fuel feed concentrations.

2. Experimental

The membrane electrode assemblies (MEA) were fabricated in house using a 'direct paint' technique to apply the catalyst layers. The active cell area is 5 cm^2. The 'catalyst inks' were prepared by dispersing the catalyst nanoparticles into appropriate amounts of Millipore water and 5% recast Nafion® solution (1100EW, Solution Technology Inc.). Then both the anode and cathode 'catalyst inks' were directly painted onto either side of a Nafion® 117 membrane. The cathode catalyst used in this study was unsupported platinum black (27 m^2/g, Johnson Matthey) at a standard loading of 7 mg/cm^2. A proprietary catalyst (UIUC-B) containing precious metals was used for the anode with a loading of 4 mg/cm^2. A carbon cloth diffusion layer (E-Tek) was placed on top of both the cathode and anode catalyst layers. Results from the testing of two MEAs are presented within this paper.

The single-cell test fixture was designed for use with formic acid and built in house. The anode/cathode flow fields were machined into conductive graphite blocks. The formic acid/humidified O_2 enters the cells graphite blocks through plastic swagelock fittings, directly into the anode/cathode sides of the graphite blocks, respectively. The MEA/carbon cloth is sandwiched between the two flow fields and sealed with 35 durometer Si gasketing. The graphite blocks were housed between two heated stainless steel blocks. Single sided PC boards, placed in between the stainless steel blocks and the backsides of the machined graphite blocks, acted as current collectors.

The MEAs were initially conditioned within the testing fixture at 60 °C with H_2/O_2 (anode/cathode) fuel cell mode for 1–2 h, while holding the cell potential at 0.6 V using a fuel cell testing station (Fuel Cell Technologies Inc.). The H_2 flow rate was set to 200 sccm, the gas stream was humidified to 75 °C prior to entering the cell, and a backpressure of 30 psig was applied. The O_2 flow rate was 100 sccm, the gas stream was humidified to 70 °C, and a backpressure of 30 psig was applied. After conditioning with H_2/O_2, cell polarization curves were obtained at 60 °C. For the cell polarization measurements, the anode fuel used was formic acid (Aldrich, 96% ACS grade). On the cathode, O_2 was supplied at a flow rate of 100 sccm without any backpressure, humidified to 70 °C.

The anode polarization curves were acquired by replacing the cathode O_2 gas stream with H_2. The anode potential was controlled with a galvanostat/potentiostat (model 273, EG&G), at a scan rate of 1 ml/min. The Pt/H_2 combination on the cathode side of the fuel cell fixture acted as a dynamic hydrogen reference electrode (DHE), as well as a high surface area counter electrode. The H_2 flow rate was maintained at a rate of 100 sccm, under a constant backpressure of 10 psig, humidified to 75 °C prior to entering the cell. Formic acid was supplied to the anode side of the fuel cell MEA, at a flow rate of 1 ml/min, acting as the working electrode for the electrochemical cell.

3. Results

Fig. 1A shows the effect of formic acid feed concentration on the cell polarization curve profile. The cell polarization curves were acquired over a broad formic acid feed concentration range 2–20 M. At 20 M formic acid, it is 75 wt.% of the total solution. There is relatively little cell activity for 2 M formic acid. The cell activity increases with feed concentration. At fuel feed concentrations at and below 10 M, there is a mass transport limitation in the supply of formic acid to the anode, as seem by the limiting current at lower cell potentials. The optimal formic acid feed concentration, as seen from the cell polarization curves, is between 10 and 20 M formic acid. The maximum current was observed in Fig. 1A was for 12 M formic acid, 134 mA/cm^2 at 60 °C. At formic acid feed concentrations of 20 M and above, the entire cell polarization curve profile drops. A key feature to note is the relatively high OCP of the cell, 0.72 V.

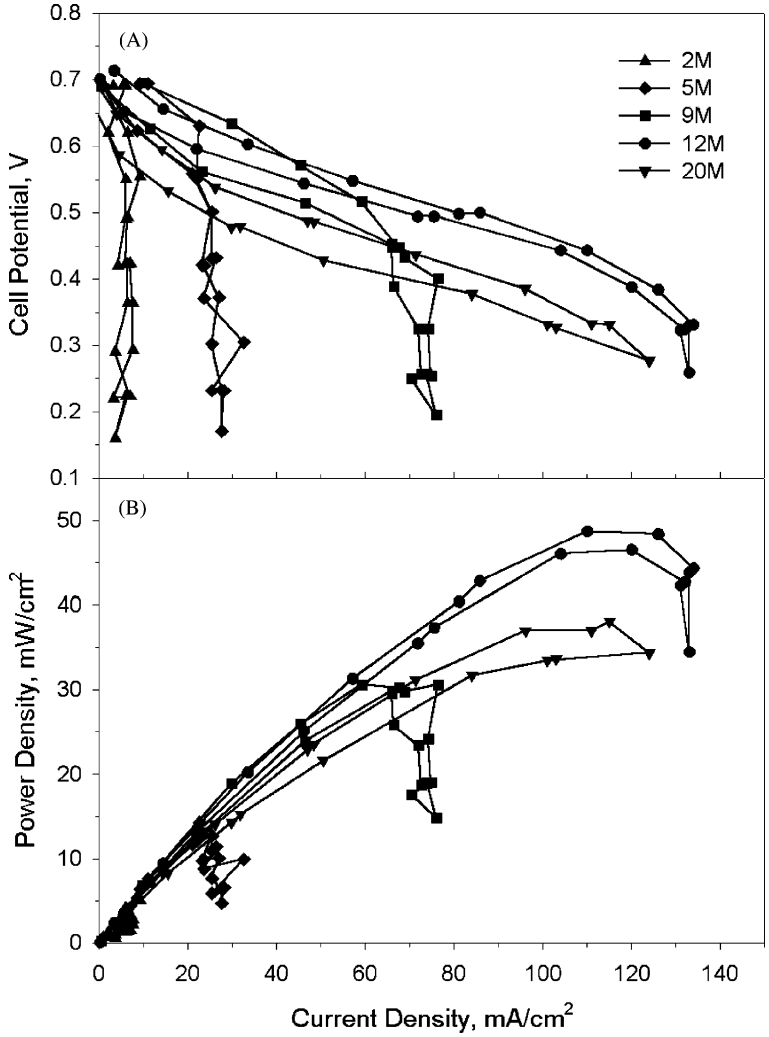

Fig. 1. Formic acid/O_2 current density vs. feed concentration at 60 °C: (A) cell potential and (B) power density curves. The formic acid flow rate to the anode was 1 ml/min. Humidified (70 °C) O_2 was supplied to the cathode at a flow rate of 100 sccm.

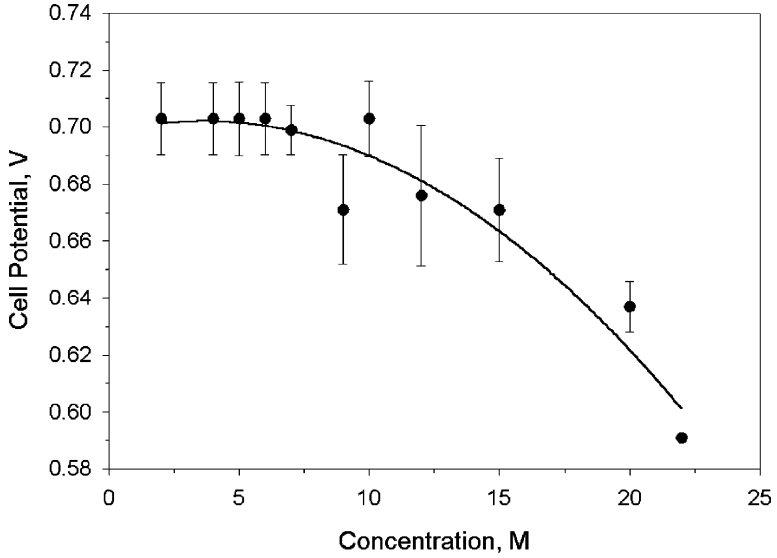

Fig. 2. Plot of formic acid feed concentration vs. OCP for the cell. The cell temperature was 60 °C. The formic acid flow rate to the anode was 1 ml/min. Humidified (70 °C) O_2 was supplied to the cathode at a flow rate of 100 sccm.

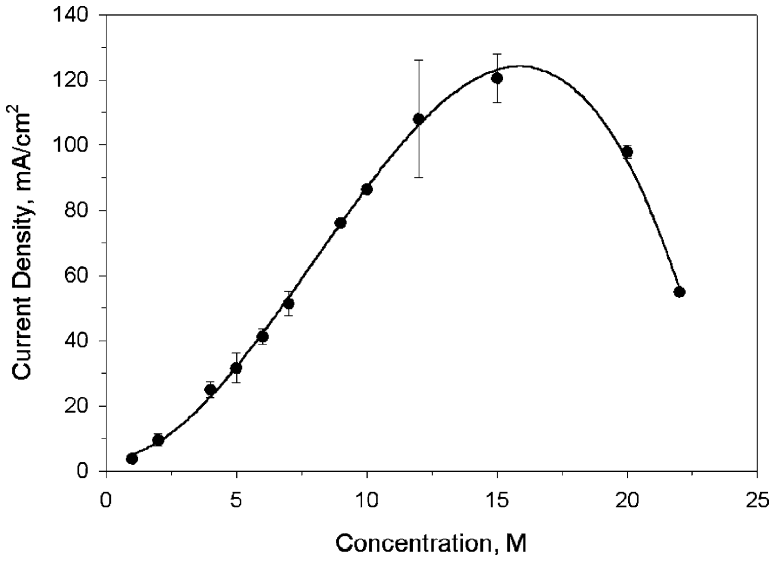

Fig. 3. Plot of formic acid feed concentration vs. current density at 0.4 V cell potential. The cell temperature was 60 °C. The formic acid flow rate to the anode was 1 ml/min. Humidified (70 °C) O_2 was supplied to the cathode at a flow rate of 100 sccm.

In Fig. 1B, the results from Fig. 1A are further processed in terms of power density for the various formic acid feed concentrations. Power density is plotted against current density. For formic acid feed concentrations below 10 M, the power density curves show an initial increase with current density, reaching a maximum value, followed by a sharp decease. The decease is due to mass transport limitations, causing fuel supply depletion. As the formic acid feed concentration is increased from 2 to 12 M the initial power density slopes follow the same general trend, prior to fuel supply depletion. For 2 M formic acid feed concentrations, a power density of 5 mW/cm^2 is attained. The maximum power density in Fig. 1B was found for 12 M formic acid, 48.8 mW/cm^2. The 20 M formic acid power density profile shows an overall loss in cell performance, by a decrease in overall power density versus current density.

Fig. 2 highlights the effects of formic acid feed concentration on the OCP of the fuel cell. At lower fuel cell feed concentrations, a maximum OCP of 0.72 V is observed. The feed concentration range investigated was from 2 to 22 M formic acid at a flow rate of 1 ml/in. As the fuel feed concentration is increased from 2 to ∼10 M formic acid, the OCP remains relatively constant. Above 10 M the OCP begins to decrease.

In Fig. 3, the effects of feed concentration on current density at 0.4 V are plotted. The formic acid feed concentration range studied was between 1 and 22 M at a flow rate of 1 ml/min. The current density was attained from cell

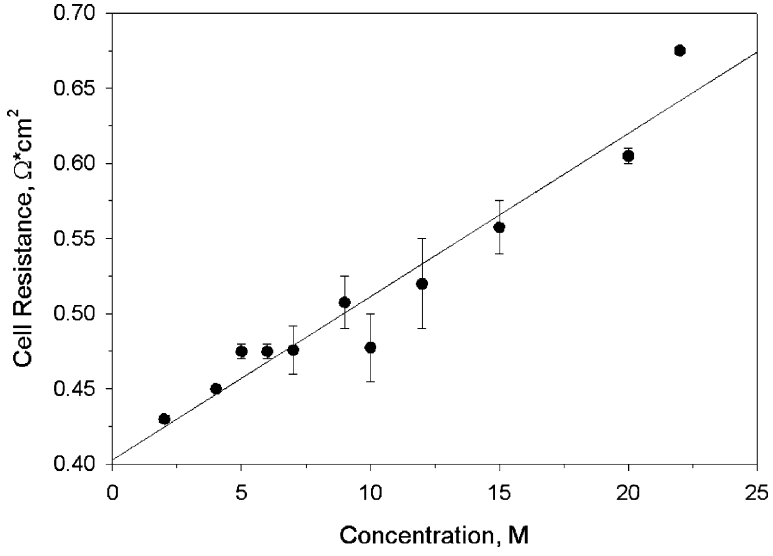

Fig. 4. Influence of the feed concentration of formic acid vs. cell resistance. The cell temperature was 60 °C. The formic acid flow rate to the anode was 1 ml/min. Humidified (70 °C) O_2 was supplied to the cathode at a flow rate of 100 sccm.

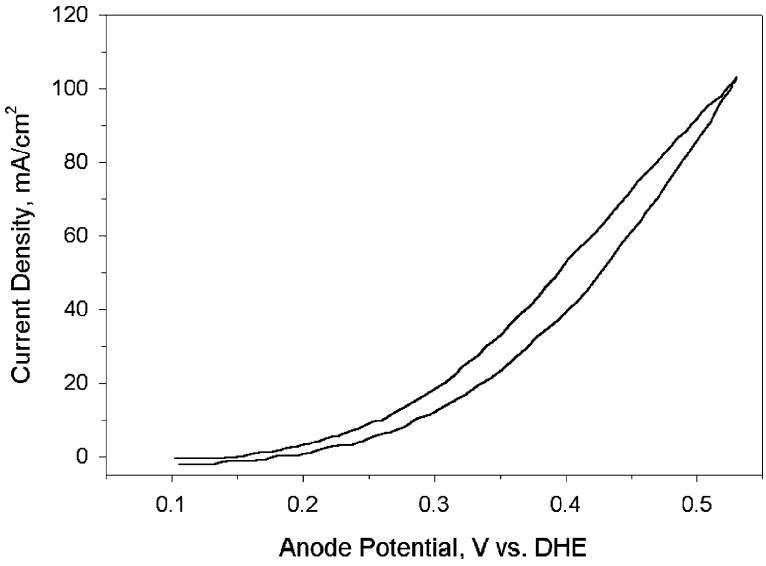

Fig. 5. Anode polarization curve of 12 M formic acid feed flowing at 1 ml/min, record at 1 mV/s. The potential has been corrected for *iR* drop. The cell temperature was 60 °C. The cathode was set-up as a dynamic hydrogen reference electrode/counter electrode: humidified (70 °C) H_2 was supplied at a flow rate of 100 sccm.

polarization curves at 0.4 V. There is very little activity at the lower fuel feed concentrations. As the feed concentration is increased there is an increase in the cell activity observed at 0.4 V. A maximum in cell activity is reached in the feed concentration range between 10 and 20 M formic acid. For feed concentrations of 20 M formic acid and higher, the cell activity begins to decrease.

Fig. 4 shows the effects of formic acid feed concentration on the high frequency cell resistance. During the cell polarization curve acquisition, the high frequency cell resistance was measured. The cell resistance steadily increased with formic acid feed concentration, from 0.43 to 0.675 Ω/cm^2 at 2 and 22 M, respectively.

Fig. 5 plots the anode polarization curve for 12 M formic acid. The anode polarization plot differs from the cell polarization plots, in that the potential is directly reference against a DHE. This removes the effects of the cathode, thereby facilitating the quantitative interpretation of the catalyst/fuel performance results. The graph shows that initial formic acid oxidation begins at about 0.15 V versus DHE.

4. Discussion

In Fig. 1A fuel cell performance was studied over a range of 2–20 M formic acid feed concentrations. The cell polarization curves measure the overall cell activity at the various anode fuel feed concentrations. The curves acquired at higher fuel feed concentrations provide clear evidence that formic acid is a viable alternative fuel for direct fuel cell applications. An OCP of 0.72 V was observed for our direct formic acid fuel cell. The typical OCP for a DMFC under similar conditions is only around 0.6 V. For our direct formic acid fuel cell, we observe about a 0.1 V increase in the OCP. The higher OCP translates into a high power density and enhanced cell efficiency at lower applied loads. Within the optimal feed concentration range, between 10 and 20 M formic acid, there is significant cell activity at high cell potentials (0.72–0.50 V), unlike that found for DMFCs.

High feed concentrations of formic acid are needed in order to obtain reasonable current densities, due to mass transport limitations. Two possible barriers hindering mass transport of formic acid to the anode might possibly be the Nafion® within the catalyst layer and/or the carbon cloth. On the other end of the feed concentration spectrum (at and above 20 M), there is a large drop in cell potential causing a negative shift in cell activity.

Fig. 1B transforms the data in Fig. 1A in terms of power density versus current density. The feed concentrations below 20 M formic acid follow the same initial power density trends. For feed concentrations below 10 M, a sharp cut off in cell activity is observed, due to mass transport limitations. While the power density curve for 20 M formic acid exhibits an overall drop in performance. The maximum power density for 12 M formic acid is 48.8 mW/cm^2 at 0.4 V. For a typical DMFC under identical conditions (1 M methanol, 60 °C, Pt/Ru), we observe a maximum power density of 51.2 mW/cm^2 at 0.27 V. If we focus on the power density at 0.4 V, 12 M formic acid out performs a typical 1 M methanol fuel cell, 48.8 mW/cm^2 versus 32.0 mW/cm^2, respectively. Showing again that formic acid is superior at higher cell potentials than methanol. We expect to eventually attain further improved cell performance, once we optimize our fuel cell system for formic acid.

The OCP for the cell was found to vary with the formic acid feed concentration (Fig. 2). The OCP is fairly constant about 0.70 V, in the feed concentration range from 2 to

~10 M. Above 10 M, the OCP begins to drop, becoming lower and lower with increased formic acid feed concentrations. At 20 M the OCP drops to 0.59 V.

Fig. 3 is a plot of the current density from Fig. 1 at 0.4 V verses feed concentration. Initially, there is a steady increase in cell activity as the formic acid feed concentration is increased. The optimal feed concentration is between 10 and 20 M. There is a loss in activity for feed concentrations at and above 20 M.

Fig. 4 shows that the high frequency cell resistance was also affected by the formic acid feed concentration. There is almost a linear increase in the cell resistance with feed concentration. The increase in cell resistance is directly linked to a decrease in overall cell conductivity. There are two possible reasons for a decrease in cell conductivity: a resistance to electron flow and/or a barrier to proton conduction.

The trends found in Figs. 2–4 are obviously linked to one another: (1) the decrease in OCP at formic acid feed concentrations above 10 M, (2) the decrease in cell polarization current densities at feed concentrations at and above 20 M, and (3) the linear increase in cell resistance with feed concentration. There are four possible reasons for the observed drop in cell performance with increased formic acid feed concentrations: (1) catalyst poisoning, (2) formic acid crossover from the anode to the cathode through the membrane, (3) diffusional barriers within the carbon cloth, and (4) dehydration of the membrane. From the cell polarization measurements (Fig. 3), the mass transport limitations of formic acid supplied to the catalyst surface require higher fuel feed concentrations, counter balancing the effects of increased cell resistance (Fig. 4). Within the feed concentration range from 2 to 10 M formic acid, the cell resistance increases slowly, therefore, having minimal effects on the OCP (Fig. 2). At fuel feed concentrations above 10 M formic acid the effects of increased cell resistance are seen in the loss of OCP, followed by the decrease in cell performance at feed concentrations at and above 20 M.

Catalyst poisoning can be ruled out since catalyst poisoning would not cause an increase in cell resistance.

There does not appear to be a strong fuel crossover component induced by the increase in formic acid feed concentration. For systems running on methanol, the fuel feed concentration is limited to 1 M, due to sever crossover from the anode to the cathode through the membrane, poisoning the cathode catalyst and causing significant losses in the high potential range performance. Scott et al. show a similar OCP for the cell versus concentration plot for methanol in Fig. 4A [16]. By comparison, Scott's results show a steady decrease in OCP values within the methanol feed concentration range of 0.1–2 M. While our results in Fig. 2 for formic acid show that the OCP is constant over the range of 2–10 M. In accordance with White's paper, the flux of formic acid through the Nafion® membrane is controlled by electrostatic interactions between the Nafion® terminal sulfate groups and the solute [15]. Formic acid partially dissociates in to $HCOO^-$ that are repelled by the sulfonic groups, hence, severely reducing the effects of crossover. Feed concentrations in excess of 15 M formic acid exhibit high cell resistance, not originating from fuel crossover, which most likely cause the drop in the OCP.

There may be some effects stemming from formic acid diffusional barriers within the carbon cloth. If diffusion of formic acid through the carbon cloth where the main limitation, according to Scott's findings, one would expect is a limiting current at higher fuel concentrations due to the increase production of carbon dioxide gas inhibiting methanol mass transport [16]. This phenomenon would not account for the decrease in the OCP, the overall drop on cell activity, or the increase in cell resistance at elevated formic acid feed concentrations.

As the formic acid feed concentration is increased, there is a dramatic increase in cell resistance. There are two possible explanations for this phenomenon: (1) a decrease in cell conductivity or (2) dehydration of the membrane. A decrease in conductivity can be ruled-out, because formic acid is an excellent electrolyte. Hence, the cell conductivity should increase with feed concentration. Dehydration of the membrane is a plausible explanation for the increase in cell resistance with feed concentration, due to the fact that the higher feed concentrations are almost completely devoid of water. A percentage of the water supplied form the fuel feed solution will be removed from the anode via electro-osmotic drag to the cathode accelerating dehydration of the membrane [17].

Weighing all the possible reasons for the observed behavior found in Figs. 2–4, dehydration of the membrane is the most probable explanation. The observed trends appear to be tied to the steady increase in cell resistance versus enhanced mass transport with feed concentration, showing the significance of membrane dehydration at fuel feed concentrations above 15 M, where there is very little water in the feed solution.

Fig. 5 is the anode polarization of 12 M formic acid on the UIUC-B catalyst. The onset of formic acid oxidation is at relatively low potential, ~0.15 versus DHE. Methanol oxidation does not begin until approximately 0.3 V versus DHE on a standard Pt/Ru catalyst. There is more than a 0.1 V enhancement in the oxidation potential of formic acid. This 0.1 V decrease in anode oxidation potential translates to the 0.1 V increase in the OCP for the cell.

5. Conclusions

The cell polarization curves in Fig. 1 clearly show that formic acid is a viable fuel for direct fuel cell systems. Within the upper cell potential range, formic acid out performs DMFCs, producing higher OCPs for the cell and current densities. Formic acid fuel cells are also not dominated by crossover, as are DMFCs, due to anodic repulsion of the formic acid by the Nafion® membranes terminal

sulfonic groups. Dehydration of the membrane becomes an issue at higher and higher formic acid feed concentrations, as seen by the increase in cell resistance, causing a decrease in cell performance. From evaluation of the cumulative trends seen from the presented results, dehydration of the membrane is the dominate factor that effects cell performance at formic acid feed concentrations of 20 M and higher.

We are only at the beginning of studying direct formic acid fuel cells. Further studies are needed to improve the understanding of the system chemistry to explain the effects of flow rate, high frequency cell resistance, catalyst chemistry, and catalyst activity stability, i.e. long term testing. Crossover measurements need to be acquired, to see if the cathode is being poisoned by formic acid at higher fuel feed concentrations, by even 1 min fraction. The fuel cell system needs to be further optimized for formic acid, looking specifically at the transport of formic acid through the carbon cloth diffusion layer and the effect of anodic repulsion versus Nafion® content within the anode catalyst layer.

Acknowledgements

We would like to thank Thomas Barnard for preparing the UIUC-B catalyst. This material is based upon work supported by the Defense Advanced Projects Research Agency under US Air Force Grant F33615-01-C-2172. The catalyst used in this work was originally developed in a project supported by the Department of Energy under Grant DEGF-02-99ER14993. Any opinions, findings, and conclusions or recommendations expressed in this publication are those of the authors and do not necessarily reflect the views of the Department of Energy, the US Air Force, or the Defense Advanced Projects Research Agency.

References

[1] F. Sauer, J. Beck, G. Schuster, G.K. Moortgat, Chemosphere: Global Change Sci. 3 (2001) 309–326.
[2] A.L. Winter, R. Fychan, R. Jones, Grass Forage Sci. 56 (2001) 181–192.
[3] US Code of Federal Regulations, 21 CFR 186.1316.
[4] US Code of Federal Regulations, 21 CFR 172.515.
[5] C. Rice, R. Masel, P. Waszczuk, A. Wieckowski, Fuel Cells for Micro Power Applications, Proceedings 40th Power Sources Conference, p. 254, 2002.
[6] B. Beden, C. Lamy, in: R.J. Gale (Ed.), Spectroelectrochemistry: Theory and Practice, Plenum Press, New York, 1988 (Chapter 5).
[7] A. Bewick, B. Pons, R. Clark, R. Hester (Eds.), Vol. XII, Wiley, London, 1985 (Chapter 1).
[8] T.D. Jarvi, E.M. Stuve, in: J. Lipkowski, P.N. Ross (Eds.), Fundamental Aspects of Vacuum and Electrocatalytic Reactions of Methanol and Formic Acid on Platinum Surfaces, Wiley, New York, 1998 (Chapter 3).
[9] N. Markovic, H. Gasteiger, P. Ross, X. Jian, I. Villegas, M. Weaver, Electrochim. Acta 40 (1995) 91.
[10] R. Parsons, T.J. VanderNoot, Electroanal. Chem. 257 (1988) 9–45.
[11] P.N. Ross, in: J. Lipkowski, P.N. Ross (Eds.), The Science of Electrocatalysis on Bimetallic Surfaces, Wiley, New York, 1998, pp. 63–66.
[12] X. Xia, T.J. Iwasita, Electrochem. Soc. 140 (1993) 2559.
[13] M. Weber, J.T. Wang, S. Wasmus, R.F.J. Savinell, Electrochem. Soc. 143 (1996) L158–L160.
[14] G.Q. Lu, A. Crown, A.J. Wieckowski, Phys. Chem. B 103 (1999) 9700.
[15] B.D. Bath, H.S. White, E.R. Scott, Anal. Chem. 72 (2000) 433–442.
[16] K. Scott, W.M. Taama, P. Argyropoulos, K. Sundmacher, J. Power Sources 83 (1999) 204–216.
[17] X. Ren, S. Gottesfeld, J. Electrochem. Soc. 148 (1) (2001) A87–A93.